ARTICLE IN PRESS

Atmospheric Environment xxx (2011) 1–9

Contents lists available at SciVerse ScienceDirect

Atmospheric Environment

journal homepage: www.elsevier.com/locate/atmosenv

Modeling Europe with CAMx for the Air Quality Model Evaluation International Initiative (AQMEII)

Uarporn Nopmongcol [a], Bonyoung Koo [a], Edward Tai [a], Jaegun Jung [a], Piti Piyachaturawat [a], Chris Emery [a], Greg Yarwood [a,*], Guido Pirovano [b,c], Christina Mitsakou [d], George Kallos [d]

[a] ENVIRON International Corporation, 773 San Marin Drive, Suite 2115, Novato, CA 94998, USA
[b] Ricerca sul Sistema Energetico (RSE), Italy
[c] Institut National de l'Environnement Industriel et de Risques (INERIS), France
[d] School of Physics, the Division of Physics of Environment and Meteorology, University of Athens, Greece

ARTICLE INFO

Article history:
Received 31 May 2011
Received in revised form
4 November 2011
Accepted 10 November 2011

Keywords:
AQMEII
Photochemical modeling
Sensitivity analysis
Decoupled direct method
Ozone
PM10
PM2.5
CAMx
MM5
WRF
MEGAN

ABSTRACT

The CAMx photochemical grid model was used to model ozone (O_3) and particulate matter (PM) over a European modeling domain for calendar year 2006 as part of the Air Quality Model Evaluation International Initiative (AQMEII). The CAMx base case utilized input data provided by AQMEII for emissions, meteorology and boundary conditions. Sensitivity of model outputs to input data was investigated by using alternate input data and changing other important modeling assumptions including the schemes to represent photochemistry, dry deposition and vertical mixing. Impacts on model performance were evaluated by comparisons with ambient monitoring data. Base case model performance for January and July 2006 exhibited under-estimation trends for all pollutants both in winter and summer, except for SO_2. SO_2 generally had little bias although some over-estimation occurred at coastal locations and this was attributed to incorrect vertical distribution of emissions from marine vessels. Performance for NOx and NO_2 was better in winter than summer. The tendency to under-predict daytime NOx and O_3 in summer may result from insufficient NOx emissions or overstated daytime dilution (e.g., too deep planetary boundary layer) or monitors that are located near sources (e.g., roadside monitors). Winter O_3 was biased low and this was attributed to a low bias in the O_3 boundary conditions. PM_{10} was widely under-predicted in both winter and summer. The poor PM_{10} was influenced by under-estimation of coarse PM emissions. Sensitivities of O_3 concentrations to precursor emissions are quantified using the decoupled direct method in CAMx. The results suggest that O_3 production over the central and southern Europe during summer is mostly NOx-limited but for a more northerly city, London, O_3 production can be limited either by NOx or VOC depending upon daily meteorological conditions.

1. Introduction

The Air Quality Model Evaluation International Initiative (AQMEII) is a collaborative study aimed at improving the state of current knowledge regarding the magnitude of uncertainties in regional air quality models for ozone (O_3) and particulate matter (PM) (Rao et al., 2011). Multiple models were applied in the AQMEII and, to promote consistent model applications and minimize uncertainties associated with use of differing inputs by each model, the AQMEII organizers made available key model input data such as emissions, boundary conditions (BCs) and meteorology. However, many models used different meteorological data, several used different BCs and a few used different emissions. In this study, we applied the Comprehensive Air Quality Model with Extensions (CAMx) photochemical grid model (ENVIRON, 2010) for the European domain using the emissions, meteorology and BCs provided by the AQMEII and in addition investigated the influence of input data, assumptions and uncertainties on CAMx model performance. In the following sections, we discuss the application of CAMx to Europe using the input data provided by AQMEII, model sensitivity analyses including use of alternate input data/assumptions, and O_3 sensitivity to precursor emissions (anthropogenic NOx and VOC).

* Corresponding author. Tel.: +1 415 899 0704; fax: 1 415 899 0707.
E-mail address: gyarwood@environcorp.com (G. Yarwood).

1352-2310/$ – see front matter © 2011 Elsevier Ltd. All rights reserved.
doi:10.1016/j.atmosenv.2011.11.023

2. Methodology

2.1. Base case modeling

Air quality modeling for the European (EU) domain and calendar year 2006 used CAMx version 5.21 to simulate physical and chemical processes governing the formation and transport of O_3 and PM (ENVIRON, 2010) with Carbon Bond 05 (CB05) gas phase chemistry (Yarwood et al., 2005). Model inputs were prepared from data provided by AQMEII supplemented by other data sources as described below. The CAMx modeling domain was defined in latitude and longitude with 207 by 287 grid cells and 23 vertical layers. The modeling domain covered most of Europe, from 15.875°W to 35.875°E and 34.5625°N to 70.4375°N, with a grid resolution of 0.125° latitude by 0.25° longitude (equivalent to about 15–20 km). The grid resolution of the CAMx domain was aligned to the emission inventory in order to avoid spatial interpolation of gridded emissions data. The extent of the CAMx domain encompasses the common grid for analysis of model results, from 15°W to 35°E and 35°N to 70°N at 0.25° resolution.

2.1.1. Meteorology

Meteorological data for calendar year 2006 were developed for AQMEII using the MM5 model (Dudhia, 1993) with 35 km resolution by the Laboratoire des Sciences du Climat et de l'Environnement (CEA) in Paris, France (Vautard et al., in press). The MM5 domain was defined in Mercator projection with 180 by 220 grid cells and 32 vertical layers with a 30 m deep surface layer. The MM5CAMx preprocessor for CAMx was used to interpolate from the Mercator projection employed by MM5 to the more finely resolved latitude–longitude coordinate system used by CAMx. CAMx employed fewer vertical layers (23) than MM5 (32) to reduce the computational burden of the air quality simulations. The CAMx vertical layers exactly matched those used in MM5 for the lowest 14 layers (up to ~1800 m) and above this altitude were aggregates of several MM5 layers. Minimum vertical diffusivity (K_v) was set to 1.0 m^2/s.

2.1.2. Emission inventory

Anthropogenic emissions for 2006 were developed by TNO Environment and Geosciences (Pouliot et al., this issue). The data consisted of annual average emissions for 10 SNAP (Selected Nomenclature for sources of Air Pollution) sectors (Visschedijk et al., 2007) on a 1/16 by 1/8° latitude-longitude grid. Major point sources were gridded, which combined sources of the same SNAP sector in each grid cell, and plume rise was accounted using layer-fractions which were constant spatially and temporally for each SNAP sector. Chemical constituents included methane (CH_4), carbon monoxide (CO), nitrogen oxides (NOx), sulfur oxides (SOx), non-methane volatile organic compounds (NMVOC), ammonia (NH_3) and particulate matter of 10 and 2.5 μm or less (PM_{10} and $PM_{2.5}$).

The Emissions Processing System version 3 (EPS3) was used to prepare emissions data for input to CAMx using temporal allocation and vertical layer distribution profiles provided by TNO for each SNAP sector. Speciation profiles for NMVOC to the CB05 chemical mechanism (Yarwood et al., 2005) were developed based on data from Passant (2002). TNO provided PM speciation profiles to allocate PM10 to sulfate (PSO4), elemental carbon (EC), primary organic carbon (POC), Sodium (Na), other PM fine, and other PM coarse. CAMx models the total mass of organic aerosol (i.e., POA for primary organic aerosols) rather than carbon mass (i.e., POC) and factors of 1.45–1.8 were applied to the POC mass to calculate POA and subtracting the mass difference from "other PM fine" to conserve total PM mass.

The 2006 anthropogenic emissions for the CAMx modeling domain are summarized by SNAP sector in Table 1 and by country or sea area in Table S1. NOx emissions are primarily from on-road and off-road mobile sources (63%) which includes marine vessels. The largest contributor to SO_2 emissions (56%) is the power generation sector. Solvent use contributes 37% and on-road mobile sources (22%) of NMVOC emissions. Agricultural sources dominate NH_3 emissions (93%). Emissions in sea areas are dominated by commercial shipping.

Biogenic emissions depend strongly on meteorology and land-cover and were estimated using the Model of Emissions of Gases and Aerosols from Nature (MEGAN; Guenther et al., 2006; Sakulyanontvittaya et al., 2008) at each hour for each grid cell. MEGAN has a global database of landcover derived from satellite data at 1 km resolution. Meteorological input data for MEGAN (i.e., temperature and solar radiation) were taken from the MM5 predictions. MEGAN estimates emissions of isoprene, methyl-butenol, terpenes, sesquiterpenes, other VOCs (OVOCs) and soil NOx.

Biomass burning emissions were estimated by the Finnish Meteorological Institute (FMI; Sofiev et al., 2010) using the fire radiative power (FRP) data product from MODIS equipped satellites. The dataset consisted of daily PM emissions for each fire gridded at 0.1° resolution. Scaling factors were provided to calculate gaseous components (CO, HCHO, NOx, NH_3, and SO_2) as ratios to PM. FMI suggested distributing emissions vertically by placing 50% of emissions below 200 m and 50% between 200 m and 1 km (Sofiev et al., 2010) but US modeling studies have used higher plume rise (ASI, 2005). Plume rise is related to the spatial extent of fires, and other factors, which are likely to differ for the conditions analyzed by FMI and the US studies. For the base case, fire plume rise was modeled by analyzing the emission inventory data to categorize the area burned by each fire and then using plume rise equations specific for fires of differing spatial extent (ASI, 2005).

Table 1
Anthropogenic emissions by SNAP sector for 2006 (metric tons/year).

	SNAP Sector	CO	NOx	NMVOC	CH4	NH3	SO2	PM10
1	Combustion in energy industries	762,912	2,903,396	120,552	774,388	5984	7,781,377	431,632
2	Non-industrial combustion	11,340,097	833,530	1,137,160	677,509	10,978	791,519	866,201
3	Combustion in manufacturing Industry	4,003,572	1,849,805	177,135	278,575	5854	1,900,364	313,757
4	Production processes	3,282,061	378,349	1,082,172	61,159	120,157	492,550	535,376
5	Energy extraction and distribution	149,083	41,399	941,238	5,595,385	930	239,703	66,655
6	Solvent use	27,422	184	4,495,530	0	9760	6766	59,816
7	Road transport	14,262,267	5,085,578	2,635,363	113,785	81,671	90,220	402,004
8	Other mobile sources	3,288,189	5,408,350	756,676	6159	3048	2,563,899	496,021
9	Waste treatment and disposal	1,582,985	30,175	118,913	8,609,183	121,147	7753	102,764
10	Agriculture	190,261	193,548	538,112	12,749,030	4,889,872	3173	412,733
	Total	38,888,849	16,724,314	12,002,851	28,865,173	5,249,401	13,877,324	3,686,959

Please cite this article in press as: Nopmongcol, U., et al., Modeling Europe with CAMx for the Air Quality Model Evaluation International Initiative (AQMEII), Atmospheric Environment (2011), doi:10.1016/j.atmosenv.2011.11.023

Emissions of sea-salt particles, including sodium, chloride, and sulfate (SO_4), were estimated from the MM5 hourly, gridded meteorology using flux equations for open ocean (Smith and Harrison, 1998; Gong, 2003) and breaking waves in the surf zone (de Leeuw et al., 2000).

Average daily emissions in January and July 2006 for each source category are summarized in Table S2.

2.1.3. Boundary/Initial conditions (BCs/ICs)

Boundary conditions (BCs) for the base case were from data provided by the European Centre for Medium-Range Weather Forecasts (ECMWF) GEMS project (http://gems.ecmwf.int). The GEMS data were a composite of two models, namely MOZART for gases and IFS for particles. EPA evaluated the GEMS BCs by comparison with climatological values and GEOS-Chem model results for North America (Schere et al., in press) and concluded generally that differences between the three data sources were within the uncertainty ranges. However, EPA recommended not using sea-salt from GEMS because concentrations were high. The SO_2 and SO_4 data from GEMs also were not recommended as they were based on simple assumptions for emissions and removal rather than a complete atmospheric transformation mechanism. Neglecting sulfur from the boundaries should not greatly affect the simulations, since SO_2/SO_4 should be strongly forced by emissions within the domain. The GEMS data did not provide PM nitrate or ammonium. For the base case, BCs were extracted from GEMS data and formatted for CAMx. Background concentrations were assumed for nitrate, ammonium, sulfate and other aerosol species missing from the GEMS data. The 2006 annual simulation was initialized on December 18, 2005, to limit the influence of the ICs on results for 2006.

2.2. Sensitivity cases

Multiple sensitivity simulations were conducted to identify the role played by different input data and assumptions. Two one-month periods, January and July, were modeled for each sensitivity case and evaluated against measurements. Information on the alternative inputs and assumptions are provided below.

2.2.1. Boundary conditions

To investigate the contrasting impacts of other data sources for BCs, we replaced the GEMS BCs with results from other global models, namely, GEOS-Chem v8–03–01 (Yantosca and Carouge, 2010) and MOZART4.6 (Emmons et al., 2010). The 2006 GEOS-Chem simulation was performed by ENVIRON using input data provided by Harvard University while the 2006 MOZART results were from the University Corporation for Atmospheric Research (UCAR, 2010).

2.2.2. Meteorology

The MM5 meteorology was replaced with WRF meteorology provided by the University of Hertfordshire (Vautard et al., in press). The WRF domain covers almost all of Europe using 269 by 249 grid cells at 18 km resolution. The projection is Lambert Conformal. The vertical domain definition has 51 vertical layers with an approximately 25 m deep surface layer. The WRF data was collapsed to 24 layers in CAMx and interpolated to the CAMx lat–lon grid. Two sensitivity tests were performed using WRF meteorology with different minimum vertical diffusivity (K_v) values of 0.1 or 0.04 m^2/s. The major impact of changing the minimum K_v is on night-time mixing in/out of the shallow surface layer in CAMx.

2.2.3. Emissions

Emission estimates by MEGAN are generally higher than those estimated by EPA's Biogenic Emission Inventory System model (Pouliot, 2008). A comparison against aircraft-based measurements suggested that MEGAN over-estimated isoprene by up to a factor of 2 (Warneke et al., 2010). A sensitivity test was conducted with the MEGAN isoprene emissions reduced by half.

As discussed above, biomass burning emissions in the base case were distributed vertically according to the plume rises reported in US studies (ASI, 2005). Satellite data analysis by FMI suggested lower plume rise, i.e., ~80% within planetary boundary layer (PBL) and most plumes are below 4 km (Sofiev et al., 2010). A sensitivity test was conducted using fire vertical profiles modified to conform better to these satellite data and FMI's recommendation.

Shipping emissions in the base case were placed in the first model layer following vertical profiles suggested by AQMEII. However, deep draft vessels which account for most of the shipping emissions have stack heights comparable to the 30 m depth of the lowest CAMx layer. A study for the Port of Los Angeles characterized the stack height for deep draft vessels as between 34 and 58 m above the waterline (SCG, 2004). A sensitivity test with shipping emissions over open water assigned 75% to the second CAMx layer (the second layer top is at 73 m.) and 25% to the first CAMx layer. However, because emissions from shipping were combined with other mobile sources, this sensitivity adjustment was applied only for grid cells characterized as 100% water meaning that in-port emissions from deep draft vessels were still assigned entirely to the surface layer.

2.2.4. Dry deposition

CAMx offers two dry deposition options: the original approach is based on the work of Wesely (1989) for gases and Slinn and Slinn (1980) for particles; and a more recent approach is based on the work of Zhang et al. (2001, 2003). The base case used the Zhang scheme with 26 land use categories and incorporates vegetation density effects via leaf area index (LAI) to scale pollutant uptake into biota. The Wesely/Slinn model is formulated for 11 land use categories. A sensitivity test was conducted using the Wesely/Slinn scheme.

2.2.5. Gas-phase chemistry

The gas-phase chemical mechanism strongly influences model predictions for oxidants and secondary PM. A sensitivity test implemented the Carbon Bond 6 (CB6) chemical mechanism (Yarwood et al., 2010) with the rate constant for OH and NO_2 measured by Mollner et al. (2010). Changes in CB6 compared to CB05 include reactions of aromatics, isoprene, ketones and production of HO_2 radical from RO_2 radicals. CB6 was used with the CB05 modeling inputs which means that some improvements (e.g., explicit treatments of propane, benzene and acetylene) were not exploited.

3. Performance evaluation

Model performance was evaluated using methods implemented in the Atmospheric Model Evaluation Tool (AMET; Appel et al., 2010).

Ambient air quality measurements from the AirBase database for Europe (EEA, 2010) were used with AMET to compute statistical metrics of model performance. Background monitors (i.e., reported as being removed from traffic and industrial sources) below 700 m elevation and with data availability exceeding 75% were included in this analysis (~1400 sites). The AirBase system classifies monitors according to location type with most of the selected stations classified as urban background, 379 as suburban background and 360

Table 2
Definitions of statistical metrics of model performance.

Metric (potential range)	Definition	
Normalized Mean Bias (-100% to $+\infty$) Normalized Mean Error (0% to $+\infty$)	$NMB = \frac{\sum_{i=1}^{N}(C_m - C_o)}{\sum_{i=1}^{N} C_o}$	$NME = \frac{\sum_{i=1}^{N}\lvert C_m - C_o\rvert}{\sum_{i=1}^{N} C_o}$
Fractional Bias (-200% to $+200\%$) Fractional Error (0% to $+200\%$)	$FB = \frac{1}{N}\sum_{i=1}^{N}\frac{(C_m - C_o)}{\left(\frac{C_o + C_m}{2}\right)}$	$FE = \frac{1}{N}\sum_{i=1}^{N}\frac{\lvert C_m - C_o\rvert}{\left(\frac{C_o + C_m}{2}\right)}$

C_o = observation.
C_m = model prediction.
N = number of data pairs (C_o, C_m).

as rural background. Statistical metrics for PM constituents were computed using data from the European Monitoring and Evaluation Program (EMEP) database (EMEP, 2010). Monthly normalized mean bias (NMB), normalized mean error (NME), fractional bias (FB) and fractional error (FE) statistics (Table 2) were calculated for January and July using paired predictions and observations. January and July were selected to represent winter and summer conditions, respectively, when air pollution events occur for different reasons. Concentration thresholds were applied to the observed data (i.e., NOx $\geq$ 0.5 ppb, $NO_2 \geq 0.5$ ppb, $O_3 \geq 5$ ppb, $SO_2 \geq 0.2$ ppb, CO $\geq$ 10 ppb, $PM_{10} \geq 1.0$ μg/m^3) to focus on conditions that exceed measurement thresholds. Table 3 reports the statistical performance metrics over all stations in the modeling domain for January and July 2006.

Overall, the base case simulation under-predicted all species except SO_2 in both January and July (Table 3). SO_2 has less than 10% bias (NMB and FB) in both months but greater than 60% error (NME and FE) indicating that the average concentrations are predicted correctly but with substantial scatter. For O_3 and CO, model performance improves in July compared to January. NOx, NO_2 and PM_{10} are substantially underestimated and performance is poor for both months with similar magnitude bias and error statistics indicating that the under-estimation trends are consistent both spatially and temporally. Analyzing the NMB and FB statistics for January by monitor location type (Table S3) shows less under-prediction tendency at rural monitors than at urban monitors for most species except O_3. January O_3 is under-predicted for both the rural and urban monitor types.

The diurnal cycle of July O_3 (Figure S1 (a)) shows that the model reproduces well the daily modulation in O_3. In contrast to July,

Table 3
Statistical metrics[a] of model performance for January and July 2006.

Sensitivity Case[b]	January MPE				July MPE				January MPE				July MPE			
	NMB	NME	FB	FE	NMB	NME	FB	FE	NMB	NME	FB	FE	NMB	NME	FB	FE
	O_3								NOx							
Base Case	−48	50	−63	70	−4.0	16	−1.9	20	−37	47	−51	74	−51	54	−75	83
BC_MOZART	3.5	34	0.2	41	4.2	16	6.3	20	−44	49	−63	80	−52	54	−77	84
BC_GEOS	−19	34	−21	44	0.3	16	2.6	20	−40	48	−58	77	−52	54	−76	84
WRF_0p1	−72	73	−110	115	−15	28	−21	40	−8.3	55	−13	70	−3.1	51	−3.2	61
WRF_0p04	−80	80	−131	134	−21	32	−29	45	8.5	65	5.5	71	5.8	53	7.0	62
Bio	−48	50	−63	70	−6.4	16	−4.8	21	−37	47	−51	74	−50	53	−74	83
Fire	−48	50	−63	70	−4.0	16	−1.9	20	−37	47	−51	74	−51	54	−75	83
Ship	−48	50	−62	70	−3.7	16	−1.6	20	−37	47	−52	74	−52	54	−77	84
Deposition	−43	46	−54	63	−6.3	16	−4.5	21	−30	47	−41	71	−47	51	−68	78
Chem_CB6	−32	40	−37	54	7.2	16	9.4	21	−39	48	−56	77	−50	53	−74	82
Combo1	4.0	35	0.6	41	4.5	16	6.6	20	−44	50	−64	80	−53	54	−78	85
Combo2	25	40	19	42	14	19	15	22	−46	51	−68	83	−52	53	−76	84
	NO_2								CO							
Base Case	−38	40	−48	61	−46	49	−62	73	−37	42	−45	63	−13	33	−11	44
BC_MOZART	−35	38	−48	62	−46	50	−63	74	−35	41	−43	62	−18	34	−17	47
BC_GEOS	−35	38	−46	60	−46	50	−62	73	−36	42	−45	62	−24	36	−24	50
WRF_0p1	−27	35	−29	53	−0.1	45	−0.3	54	−17	41	−20	57	64	76	48	62
WRF_0p04	−25	35	−25	52	8.5	46	8.5	53	−4.5	44	−7.1	56	91	99	61	71
Bio	−38	40	−48	61	−45	49	−61	72	−37	42	−45	63	−15	33	−14	45
Fire	−38	40	−48	61	−46	49	−62	73	−37	42	−45	63	−12	33	−10	44
Ship	−38	40	−49	61	−47	50	−63	74	−37	42	−46	63	−13	33	−11	44
Deposition	−23	33	−30	53	−41	46	−53	68	−37	42	−45	63	−12	33	−11	44
Chem_CB6	−35	38	−46	60	−45	49	−60	72	−38	43	−47	64	−25	35	−26	50
Combo1	−35	39	−49	62	−47	50	−64	74	−35	41	−43	62	−17	34	−16	47
Combo2	−34	38	−49	63	−46	49	−62	73	−37	42	−45	62	−30	38	−33	53
	SO_2								PM_{10}							
Base Case	1.1	61	0.4	68	9.1	60	6.9	64	−38	51	−47	73	−44	46	−59	64
BC_MOZART	2.3	61	1.8	68	8.6	60	6.5	64	−33	52	−39	71	−49	51	−68	72
BC_GEOS	3.2	62	3.0	68	10	60	7.7	64	−35	53	−42	73	−52	53	−72	76
WRF_0p1	−5.3	64	−5.8	71	42	85	31	72	−34	53	−42	73	−21	35	−23	48
WRF_0p04	−5.3	66	−6.2	73	41	87	31	73	−34	54	−41	74	−18	35	−19	47
Bio	1.2	61	0.4	68	8.9	60	6.9	64	−38	51	−47	73	−44	46	−59	65
Fire	1.2	61	0.4	68	9.2	60	7.1	64	−38	51	−47	73	−43	45	−58	64
Ship	1.0	61	0.1	68	9.1	60	6.8	64	−38	51	−47	73	−44	46	−59	64
Deposition	5.7	64	4.5	69	8.6	59	6.5	64	−9.0	56	−12	65	−34	38	−43	52
Chem_CB6	14	68	12	70	20	65	15	65	−28	52	−33	69	−38	41	−50	57
Combo1	2.0	61	1.5	68	8.7	60	6.4	64	−33	52	−39	71	−48	50	−66	71
Combo2	15	68	14	69	18	64	14	64	−23	54	−26	68	−43	45	−57	63

[a] See Table 2 for definitions of the statistical metrics.
[b] BC_MOZART = replacing GEMS BCs with MOZART BCs; BC_GEOS = replacing GEMS BCs with GEOS-Chem BCs; WRF_0p1 = replacing MM5 with WRF using minimum K_v of 0.1; WRF_0p04 = similar to WRF_0p1 but with minimum K_v of 0.04; Bio = decreasing biogenic isoprene emissions by half; Fire = reducing vertical plume heights of fire emissions; Ship = placing 75% of shipping emissions into 2nd model layer; Deposition = using Wesely/Slinn dry deposition scheme; Chem_CB6 = using CB6 gas-phase chemistry; Combo1 = BC_MOZART + Fire + Ship; Combo2 = Combo1 + Bio + CB6.

January O_3 performance is poor showing consistent under-predictions. The diurnal cycle of January O_3 (Figure S1 (a)) shows that the model reproduces the daily modulation in O_3 but with an offset due to a consistent low bias. Since O_3 production by atmospheric chemistry is generally suppressed in winter, O_3 transport from the model boundaries (i.e., BCs) is expected to be the dominant factor in causing the low bias for O_3 in January. Both MOZART and GEOS-Chem BCs improve January O_3 performance significantly with the FB bias decreasing from −63% (base case) to 0.2% (MOZART) and −21% (GEOS-Chem) (Table 3). The effects of changing BCs are less evident in July indicating that the low bias in the base-case O_3 BCs is a winter problem.

In contrast to O_3, NOx performance is fairly good at rural stations in January but NOx at urban stations is under-predicted in both January and July (Table S3) and in July CAMx predicted much lower daytime NOx than observed (Figure S2 (a)). These problems may stem from model deficiencies, such as insufficient NOx emissions or overstated daytime dilution (e.g., too deep planetary boundary layer) or urban monitors that are located near sources (e.g., roadside monitors). WRF meteorology substantially changed model performance in both months, particularly for NOx. WRF estimated shallower boundary layers than MM5 and led to higher surface NOx concentrations. With WRF meteorology, NOx has −13% low bias (NMB and FB) compared to −75% low bias (FB) in the base case (Table 3). The diurnal cycles in the WRF sensitivity simulations (Figure S2) have higher night-time NOx and lower night-time O_3 than the base case. Ground-level O_3 at night is removed by reaction with NO (to form NO_2) and deposition, and can be replenished from higher-layer O_3. Night-time concentrations of NOx and O_3 were sensitive to the minimum vertical diffusion coefficient (K_v, set to 0.04 m^2/s or 0.1 m^2/s) but were not systematically better in either sensitivity test. The WRF meteorology also resulted in higher CO and PM_{10} concentrations in the surface layer than the base case (Table 3).

SO_2 performance shows positive bias at most coastal stations (e.g., around the English Channel and North Sea) while the modeled and observed concentrations are in a fairly good agreement inland suggesting that contributions from ship emissions to surface SO_2 might be over-estimated (Figure S3). A likely reason for SO_2 over-estimation at coastal locations is that all ship emissions were placed in the first model layer. As discussed above, many large vessels have sufficient stack height to release emissions into the second model layer. However, model results were insensitive to using an alternate vertical distribution of shipping emissions. This result may be due to limitations in the sensitivity test which could only move shipping emissions into the second layer for grid cells over open water.

Model performance also was relatively insensitive to changing the vertical distribution of fire emissions because both vertical distributions placed most of the fire emissions within the planetary boundary layer.

Reducing biogenic isoprene emissions has small impacts to model performance in July, and the impacts mainly occur in the southern European countries (e.g., Italy and Spain). January model performance is insensitive to this change which is expected because of low biogenic emissions during winter.

Model results are relatively sensitive to the dry- deposition scheme chosen. The Wesely/Slinn dry deposition model tends to generate higher O_3 deposition rates than the Zhang model in summer, which overall leads to lower surface O_3 concentrations. This effect is observed in our July results, but only caused 2–3% change in bias. In contrast, the Wesely/Slinn scheme increases winter O_3 and improves FB by 9%. The deposition algorithms for aerosols in the two schemes have similar formulations, but parameterizations used in the Zhang scheme result in higher deposition velocity for sub-micron aerosols, especially over rough vegetated surfaces. The Wesely/Slinn scheme improves the FB of PM_{10} from −59% to −43% in summer and from −47% to −12% in winter. However, since emissions of PM_{10} are uncertain (discussed below), our interpretation of this result is limited to a finding of sensitivity to deposition scheme rather than any conclusion that one scheme is more accurate than another.

CB6 gas-phase chemistry improves January O_3 and PM performance considerably by increasing surface concentrations. January O_3 has −37% FB low bias compared to −63% in the base case. July O_3 and PM predictions also increase. Inorganic species, such as CO and SO_2, are also affected because of changes in oxidant availability. Although PM_{10} performance improves, it is still greatly under-estimated. Figure S4 shows that $PM_{2.5}$ performance is fairly good, especially in July, suggesting that the poor PM_{10} performance is primarily due to under-estimation of coarse material mass which suggests emission inventory problems. Analysis of PM_{10} and speciated components of PM using EMEP data (Figure S5) confirms that CAMx could not reproduce PM_{10} episodes, showing a mean low bias of 13.0 μg/m^3 in January at rural EMEP stations. The combined inorganic secondary PM species (i.e., PSO_4, PNO_3, PNH_4) measured are generally less than 5 μg/m^3 (compared to 20–40 μg/m^3 of total PM_{10}) and the model could reproduce most of their mass, especially for PNO_3. This analysis suggests that emissions of coarse PM were underestimated.

Different inputs and assumptions affect model performance to different extents and depending upon pollutant. BCs and meteorology appear to impact overall model performance the most. Pollutants affected by long-range transport, i.e., O_3, CO and PM, were most affected by BCs and both MOZART and GEOS-Chem improved the performance for winter O_3 compared to the base case. In constructing a new base case simulation for emission sensitivity analysis, two model configurations with combinations of changes were selected and tested. The first configuration (combo1) incorporates MOZART BCs and changes in vertical distributions of fire and ship emissions. While changes to fire and ship emissions had small impacts on model performance, the changes are considered appropriate thus included. The second configuration (combo2) included the changes made in combo1 plus changes to biogenic isoprene emissions and CB6 chemistry. The MPE results for these two configurations are presented in Table 3 and Table S3. The performance varies by pollutant and by season. Both configurations improve O_3 performance in January considerably because of the MOZART BCs while combo2 predicts higher O_3due to CB6.

4. HDDM sensitivity analysis

The traditional approach to sensitivity analysis may be called the brute force method (BFM) where model simulations are repeated with different model inputs (as demonstrated earlier). For example, reducing biogenic VOC emissions reduced domain-wide O_3 in summer but produced negligible change in domain-wide O_3 in winter (Table 3). While the BFM is easy to apply and interpretation of the result is straightforward, the method is computationally demanding and susceptible to numerical uncertainty for small perturbations. The Decoupled Direct Method (DDM) offers an alternative to the traditional BFM by directly solving sensitivity equations derived from the governing equations of the model (Dunker, 1984; Dunker et al., 2002). The higher-order DDM (HDDM) adds the capability in CAMx for second-order sensitivity coefficients (Koo et al., 2007) which is used to understand non-linear responses and interactions between first-order sensitivities (Hakami et al., 2003, 2004; Cohan et al., 2005).

In this work, HDDM was applied to the combo1 and combo2 scenarios for a 15-day July episode (July 16–28 with two spin-up days) selected because high O_3 occurred in several major cities. First- and second-order sensitivities were computed for O_3 to domain-wide anthropogenic NOx and VOC emissions. The analysis focuses on the combo1 scenario because the results of combo2 are similar to those of combo1. Fig. 1 shows episode average hourly O_3 concentrations and the zero-out contribution (ZOC) of domain-wide anthropogenic NOx and VOC emissions at 11:00 GMT which corresponds to noon in British Summer Time (London) or 1 PM in Central European Summer Time (Milano). The ZOC of an emission source is defined as the amount by which concentrations would be reduced if that source was completely removed (i.e., zeroed out). Model response of concentrations to perturbations in input parameters can be approximated using Taylor series expansions:

$$C - C_0 = p_i S_i^{(1)} + p_j S_j^{(1)} + \frac{1}{2} p_i^2 S_i^{(2)} + \frac{1}{2} p_j^2 S_j^{(2)} + p_i p_j S_{ij}^{(2)} \quad (1)$$

$$S_i^{(1)} = \frac{\partial C}{\partial p_i}\Big|_{p_i=0}$$

$$S_{ij}^{(2)} = \frac{\partial^2 C}{\partial p_i \partial p_j}\Big|_{p_i=0;p_j=0}$$

where C–C_0 represents the concentration change due to simultaneous perturbation in two input parameters (i and j) by fractions p_i and p_j. Then, ZOC is calculated as follows:

$$\mathrm{ZOC(NOx)} = C_0 - C(p_{\mathrm{NOx}} = -100\%; p_{\mathrm{VOC}} = 0) = S_{\mathrm{NOx}}^{(1)} - \frac{1}{2} S_{\mathrm{NOx}}^{(2)} \quad (2)$$

$$\mathrm{ZOC(VOC)} = C_0 - C(p_{\mathrm{VOC}} = -100\%; p_{\mathrm{NOx}} = 0) = S_{\mathrm{VOC}}^{(1)} - \frac{1}{2} S_{\mathrm{VOC}}^{(2)} \quad (3)$$

In central and southern Europe, anthropogenic NOx contributions to O_3 are much higher than anthropogenic VOC contributions indicating that O_3 formation is mostly NOx-limited. This is primarily due to abundant biogenic VOC emissions in the region (Figure S6). Fig. 2 decomposes the source contributions of domain-wide anthropogenic NOx and VOC emissions to daily maximum O_3 concentrations in the grid cells corresponding to London, Paris, Barcelona, Athens and Milano. All the sites generally show positive contributions of anthropogenic NOx and VOC with ZOC(NOx) greater than ZOC(VOC). Contributions of cross sensitivity are

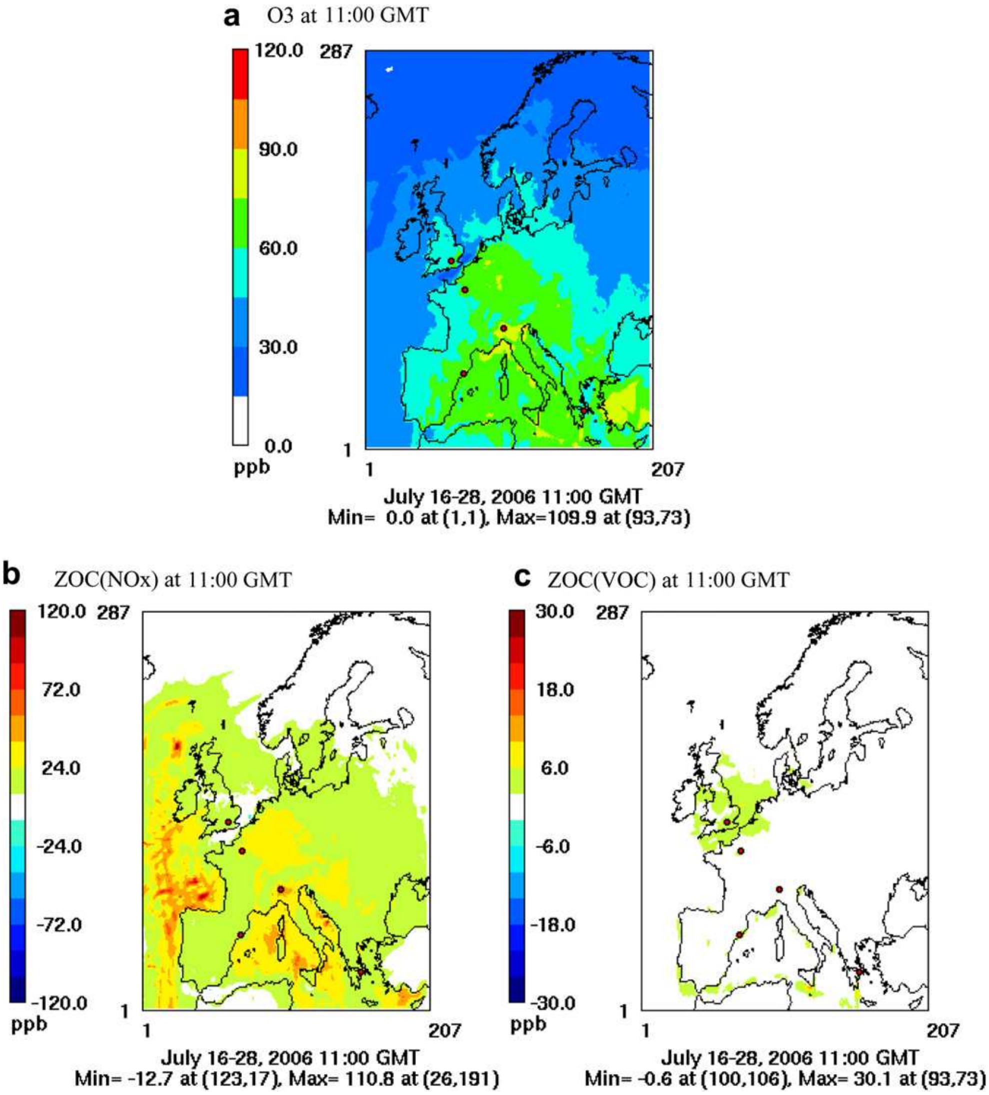

Fig. 1. Episode average hourly ozone concentrations and zero-out contributions (ZOC) estimated by HDDM at 11:00 GMT. ZOC(NOx) and ZOC(VOC) are computed by Eqs. (2) and (3), respectively. Red dots correspond to London, Paris, Milano, Barcelona, and Athens (from top to bottom).

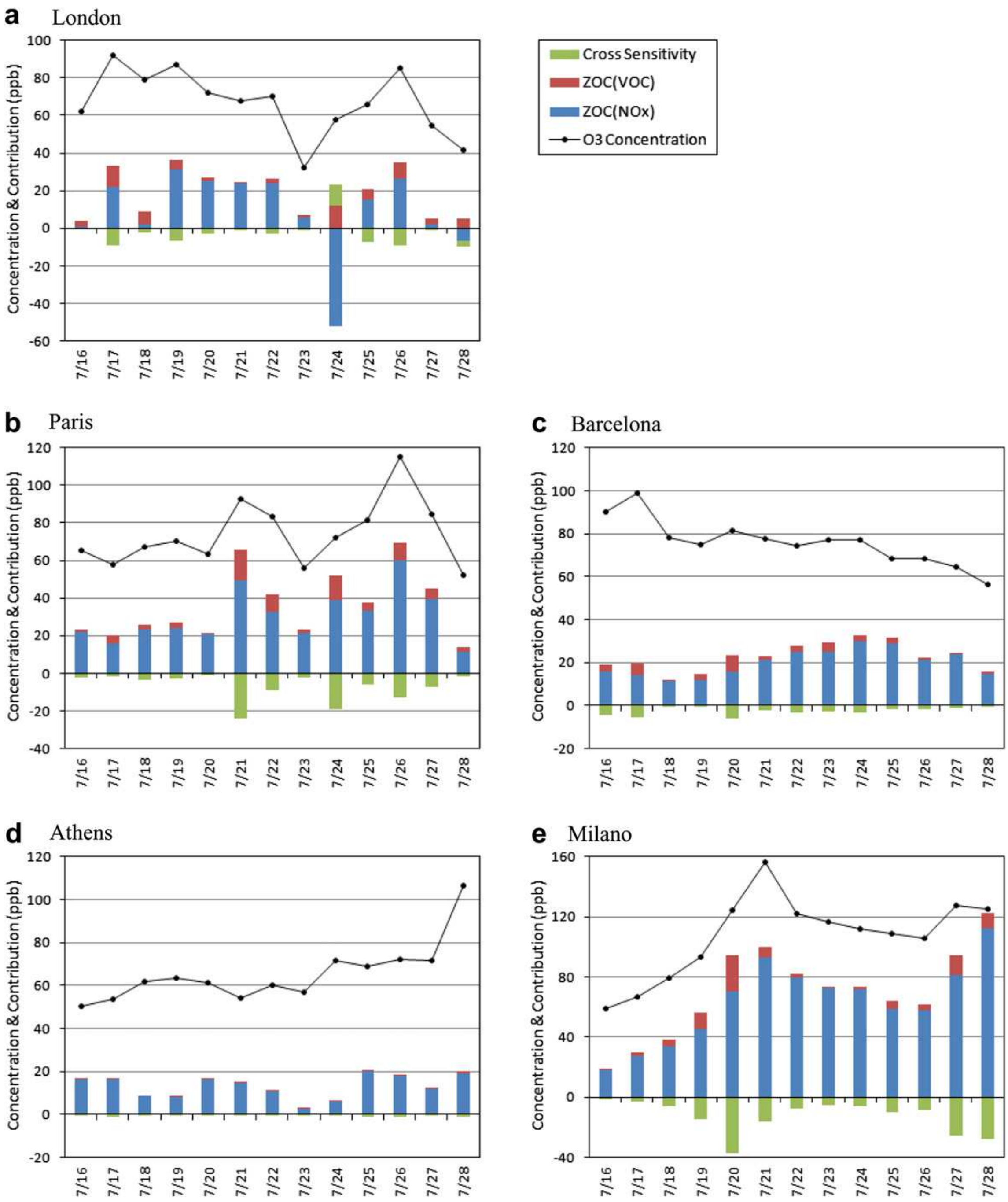

Fig. 2. Daily maximum hourly ozone concentrations and zero-out source contributions estimated by HDDM at London, Paris, Barcelona, Athens, and Milano. ZOC(NOx) and ZOC(VOC) are computed by Eqs. (2) and (3), respectively. Contribution of cross sensitivity $= -S^{(2)}_{\mathrm{NOx,VOC}}$.

mostly negative meaning that O_3 sensitivity to NOx emissions decreases as VOC emissions are reduced and vice versa. The source contributions do not sum to the modeled O_3 concentrations because biogenic emissions, boundary conditions, fires, and higher-order nonlinear interactions also play a role. Contributions from these other sources account for significant portions of O_3 concentrations at Athens and Barcelona.

London exhibits large day-to-day variations in the source contributions to daily maximum O_3, e.g., the anthropogenic NOx emissions contribution is negative on July 24 and positive on July 26. Fig. 3 shows O_3 isopleth diagrams, constructed using Eq. (1), for daily maximum O_3 concentrations at London on July 24 and 26. The response surfaces show markedly different patterns between the two days. On July 24, O_3 production at the site is clearly VOC-limited whereas July 26 is close to the ridge line dividing NOx-limited and VOC-limited conditions. This change in the chemical regime resulted from different meteorology which caused higher NOx concentrations on July 24 ($\sim$10 ppb at the hour of peak O_3) than on July 26 ($\sim$5 ppb). Fig. 3(b) indicates that if actual NOx emissions were higher than reported in the inventory, it could result shifting from the NOx-limited regime to the VOC-limited regime. At Milano, contributions of anthropogenic NOx emissions are consistently positive and large, and the O_3 isopleths for episode average daily maximum O_3 clearly show NOx-limited condition

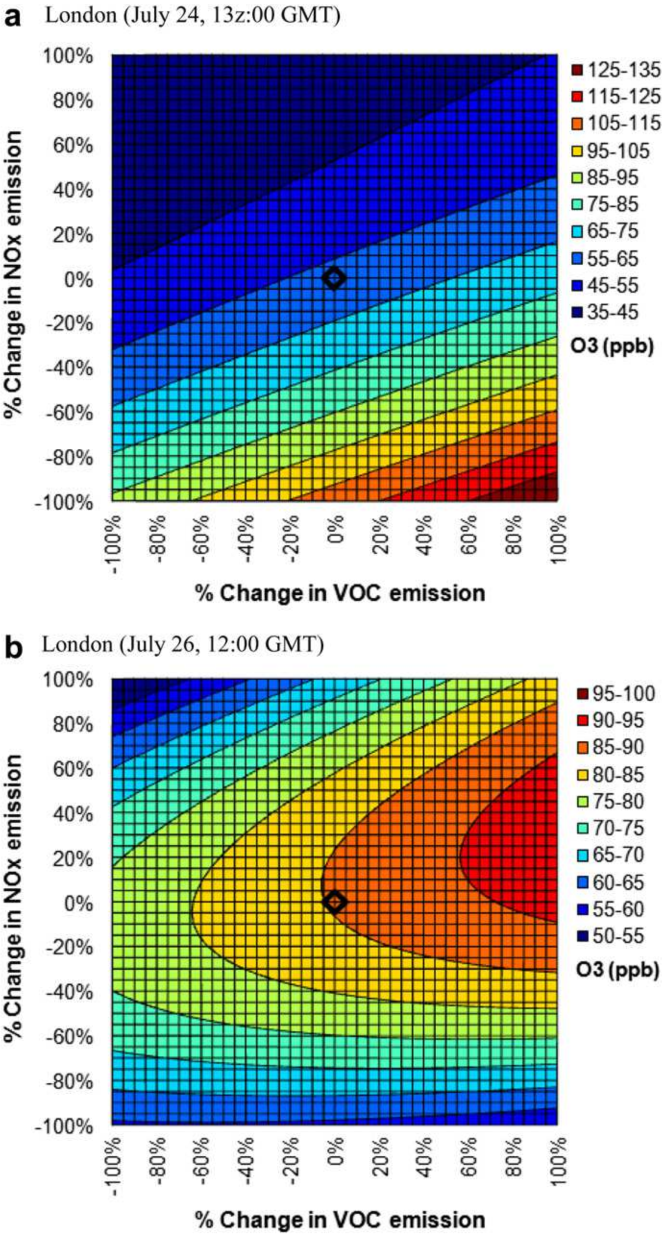

Fig. 3. Ozone isopleths constructed using the first- and second-order sensitivity coefficients (Eq. (1)) at London (July 24, 13:00 GMT & July 26, 12:00 GMT).

(Figure S7). It would require significant increases (60% or larger) in anthropogenic NOx emissions to change the chemical regime of O_3 formation at Milano from NOx-limited to VOC-limited.

5. Conclusions

CAMx modeling for the EU domain was completed for 2006 using input data for emissions, meteorology and BCs developed by AQMEII. Model performance for January and July exhibited under-estimation trends for all pollutants both in winter and summer, except for SO_2. SO_2 generally had little bias although some over-estimation occurred at coastal locations and this was attributed to incorrect vertical distribution of emissions from marine vessels. Performance for NO_X and NO_2 was better in winter than summer. The tendency to under-predict daytime NOx and O_3 in summer may result from insufficient NOx emissions or overstated daytime dilution (e.g., too deep planetary boundary layer) or urban monitors that are located near sources (e.g., roadside monitors). Winter O_3 was biased low and this was attributed to a low bias in the O_3 boundary conditions. PM_{10} was widely under-predicted in both winter and summer. The poor PM_{10} was influenced by under-estimation of coarse PM emissions. Model performance evaluation could be improved by more refined segregation of monitoring data by location type (e.g., segregating urban roadside monitors.)

The AQMEII approach to applying many models was to promote use of consistent data sources (e.g., emissions, BCs) and minimize uncertainties associated with use of differing inputs by each model. However, most models are using different meteorological data, several are using different BCs and a few are using different emissions. AQMEII is evaluating the ensemble of predictions from all models applied for Europe and may not be able to untangle the consequences of differing input data and assumptions. To investigate the influence of input data, assumptions and uncertainties on model performance for the EU domain, multiple simulations were conducted first to identify the role played by different input data. Alternate inputs and model configurations tested include BCs from alternate global models (GEOS-Chem and MOZART), alternate meteorological conditions (from WRF), reduced MEGAN isoprene emissions, modified vertical distributions for fire and shipping emissions, and alternate dry deposition (Wesely/Slinn) and chemistry (CB6) schemes. The results show that the underlying boundary conditions, emission inventory and metrological input data play a crucial role in the air quality model performance. Modeling the response to emission changes over time, i.e., modeling different years that are separated by emission reductions in response to control strategies, would be valuable for separating the influences of meteorology from emissions and boundary conditions on model performance.

Sensitivity analysis using HDDM was conducted to evaluate O_3 sensitivity (at second-order) to domain-wide anthropogenic precursor emissions (NOx and VOC). The results suggest that O_3 production over the central and southern Europe during summer is mostly NOx-limited. Combining the first- and second-order sensitivity coefficients enables construction of O_3 isopleths diagrams which can be used to determine the robustness of the chemical regime of O_3 formation (NOx-limited or VOC-limited) in a region. This analysis was performed for London, Paris, Barcelona, Athens and Milano. Cities in southern Europe were consistently NOx-limited but London changed between NOx-limited and VOC-limited from day to day.

Acknowledgement

This study was supported by Coordinating Research Council Atmospheric Impacts Committee (CRC Project A-75). The authors thank Charles Chemel for providing the WRF data.

Appendix. Supplementary data

Supplementary data associated with this article can be found in the online version, at doi:10.1016/j.atmosenv.2011.11.023.

References

Air Sciences, Inc., 2005. 2002 Fire Emission Inventory for the WRAP Region – Phase II, Prepared for the Western Governors Association/WRAP by Air Sciences, Inc., Denver, CO.
Appel, W., Gilliam, R.C., Davis, N., Zubrow, A., Howard, S.C., 2010. Overview of the atmospheric model evaluation tool (AMET) v1.1 for evaluating meteorological and air quality models. Environmental Modelling and Software 26, 434–443.
de Leeuw, G., Neele, F.P., Hill, M., Smith, M.H., Vignati, E., 2000. Production of sea spray aerosol in the surf zone. Journal of Geophysical Research 105, 29,397–29,409.

Cohan, D.S., Hakami, A., Hu, Y.T., Russell, A.G., 2005. Nonlinear response of ozone to emissions: source apportionment and sensitivity analysis. Environmental Science and Technology 39, 6739–6748.
Dudhia, J., 1993. A nonhydrostatic version of the Penn State/NCAR Mesoscale model: Validation tests and simulation of an Atlantic cyclone and cold front. Monthly Weather Review 121, 1493–1513.
Dunker, A.M., 1984. The decoupled direct method for calculating sensitivity coefficients in chemical kinetics. Journal of Chemical Physics 81 (5), 2385–2393.
Dunker, A.M., Yarwood, G., Ortmann, J.P., Wilson, G.M., 2002. The decoupled direct method for sensitivity analysis in a three-dimensional air quality model – implementation, accuracy, and efficiency. Environmental Science and Technology 36 (13), 2965–2976.
Emmons, L.K., Walters, S., Hess, P.G., Lamarque, J.-F., Pfister, G.G., Fillmore, D., Granier, C., Guenther, A., Kinnison, D., Laepple, T., Orlando, J., Tie, X., Tyndall, G., Wiedinmyer, C., Baughcum, S.L., Kloster, S., 2010. Description and evaluation of the model for ozone and related chemical tracers, version 4 (MOZART-4). Geoscientific Model Development 3, 43–67. doi:10.5194/gmd-3-43-2010.
ENVIRON, 2010. User's guide to the Comprehensive Air Quality Model with Extensions (CAMx). Version 5.2. Available at: http://www.camx.com.
European Environment Agency, 2010. AirBase – The European air quality database. Available at: http://www.eea.europa.eu/data-and-maps/data/airbase-the-european-air-quality-database.
European Monitoring and Evaluation Program, 2010. EMEP particulate matter data. Available at: http://tarantula.nilu.no/projects/ccc/emepdata.html.
Gong, S.L., 2003. A parameterization of sea-salt aerosol source function for sub- and super-micron particles. Global Biogeochemical Cycles 17, 1097–1104.
Guenther, A., Karl, T., Harley, P., Wiedinmyer, C., PalmerGeron, C., 2006. Estimates of global terrestrial isoprene emissions using MEGAN (Model of Emissions of Gases and Aerosols from Nature). Atmospheric Chemistry and Physics 6, 3181–3210.
Hakami, A., Odman, M.T., Russell, A.G., 2003. High-order, direct sensitivity analysis of multidimensional air quality models. Environmental Science and Technology 37 (11), 2442–2452.
Hakami, A., Odman, M.T., Russell, A.G., 2004. Nonlinearity in atmospheric response: a direct sensitivity analysis approach. Journal of Geophysical Research-Atmospheres 109 (D15) Art. No. D15303.
Koo, B., Yarwood, G., Cohan, D.S., 2007. Incorporation of high-order decoupled direct method (HDDM) sensitivity analysis capability into CAMx, Prepared for Texas Commission on Environmental Quality.
Mollner, A.K., Valluvadasan, S., Feng, L., Sprague, M.K., Okumura, M., Milligan, D.B., Bloss, W.J., Sander, S.P., Martien, P.T., Harley, R.A., McCoy, A.B., Carter, W.P.L., 2010. Rate of gas phase association of hydroxyl radical and nitrogen dioxide. Science 330, 646.
Passant, N.R., 2002. Speciation of UK emissions of non-methane volatile organic compounds. AEA Technology Report ENV-0545, Culham, Abingdon, United Kingdom.
Pouliot, G., Pierce, T., van der Gon, H.D., Schapp, M., Moran, M., Nopmongcol, U. Comparing emission inventories and model-ready emission datasets between Europe and North America for the AQMEII project. Atmospheric Environment, this issue.
Pouliot, G., 2008. A Tale of two models: a comparison of the biogenic emission inventory system (BEIS3.14) and the model of emissions of gases and aerosols from Nature (MEGAN 2.04). Presented at 7th Annual CMAS Conference, Chapel Hill, NC, 6–8 October.
Rao, S.T., Galmarini, S., Puckett, K., 2011. Air quality model evaluation International Initiative (AQMEII): advancing the state of the science in regional photochemical modeling and its applications. Bulletin of the American Meteorological Society 92, 23–30.
Sakulyanontvittaya, T., Duhl, T., Wiedinmyer, C., Helmig, D., Matsunaga, S., Potosnak, M., Milford, J., Guenther, A., 2008. Monoterpene and sesquiterpene emission estimates for the United States. Environmental Science and Technology 42, 1623–1629.
Schere, K., Flemming, J., Vautard, R., Chemel, C., Colette, A., Hogrefe, C., Bessagnet, B., Meleux, F., Mathur, R., Roselle, S., Hu, R.-M., Sokhi, R.S., Rao, S.T., Galmarini, S. Trace gas/aerosol boundary concentrations and their impacts on continental-scale AQMEII modeling domains. Atmospheric Environment, in press.
Slinn, S.A., Slinn, W.G.N., 1980. Predictions for particle deposition on natural waters. Atmospheric Environment 24, 1013–1016.
Smith, M.H., Harrison, N.M., 1998. The sea spray generation function. Journal of Aerosol Science 29 (Suppl. I), S189–S190.
Sofiev, M., Hakkarainen, J., Vankevich R., 2010. European fire emission data for 2006 for the AQMEII simulations. Presented at the second AQMEII workshop, Torino, Italy, 26 September 2010.
Starcrest Consulting Group, LLC., 2004. Port-Wide Baseline Air Emissions Inventory. Prepared for the Port of Los Angeles, California.
UCAR, 2010. MOZART-4 results. Data located at: <http://www.acd.ucar.edu/wrf-chem/mozart.shtml> (accessed on December 2010).
Vautard, R., Moran, M.D., Solazzo, E., Gilliam, R.C., Matthias, M., Bianconi, R., Chemel, C., Ferreira, J. Geyer, N., Hansen, A.B., Jericevic. A., Prank, M., Segers, A., Silver, J.D., Werhahn, J., Wolke, R., Rao, ST, Galmarini, S. Evaluation of the meteorological forcing used for the air quality model evaluation International Initiative (AQMEII) air quality simulations, Atmospheric Environment, in press.
Visschedijk, A.J.H., Zandveld, P., Denier van der Gon, H.A.C., 2007. A high resolution gridded European emission database for the EU integrated project GEMS, TNO, Apeldoorn, Netherlands, TNO-report 2007-A-R0233/B.
Warneke, C., De Gouw, J.A., Del Negro, L., Brioude, J., McKeen, S., Stark, H., Kuster, W.C., Goldan, P.D., Trainer, M., Fehsenfeld, F.C., Wiedinmyer, C., Guenther, A.B., Hansel, A., Wisthaler, A., Atlas, E., Holloway, J.S., Ryerson, T.B., Peischl, J., Huey, L.G., Case Hanks, A.T., 2010. Biogenic emission measurement and inventories determination of biogenic emissions in the eastern United States and Texas and comparison with biogenic emission inventories. Journal of Geophysical Research 115, 21. doi:10.1029/2009JD012445.
Wesely, M.L., 1989. Parameterization of surface Resistances to gaseous dry deposition in regional-scale numerical models. Atmospheric Environment 23, 1293–1304.
Yantosca, B., Carouge, C., 2010. GEOS–Chem v8–03–01 online user's guide. http://acmg.seas.harvard.edu/geos/doc/man/.
Yarwood, G., Rao, S., Yocke, M., Whitten, G., 2005. Updates to the Carbon Bond Chemical Mechanism: CB05. report, Rpt. RT-0400675. US EPA, Res. Tri. Park.
Yarwood, G., Whitten, G.Z., Jung, J., 2010. Development, evaluation and testing of version 6 of the carbon Bond chemical mechanism (CB6), Final Report prepared for Texas Commission on Environmental Quality, September.
Zhang, L., Gong, S., Padro, J., Barrie, L., 2001. A size-segregated particle dry deposition scheme for an atmospheric aerosol module. Atmospheric Environment 35, 549–560.
Zhang, L., Brook, J.R., Vet, R., 2003. A revised parameterization for gaseous dry deposition in air-quality models. Atmospheric Chemistry and Physics 3, 2067–2082.

Please cite this article in press as: Nopmongcol, U., et al., Modeling Europe with CAMx for the Air Quality Model Evaluation International Initiative (AQMEII), Atmospheric Environment (2011), doi:10.1016/j.atmosenv.2011.11.023